Received: 23 October 2022 | Revised: 10 March 2023 | Accepted: 30 March 2023

DOI: 10.1111/cas.15839

Cancer Science WILEY

ORIGINAL ARTICLE

# *Clostridium butyricum* inhibits epithelial–mesenchymal transition of intestinal carcinogenesis through downregulating METTL3

Kexin Zhang | Yue Dong | Mengfan Li | Wanru Zhang | Yiyun Ding | Xin Wang | Danfeng Chen | Tianyu Liu | Bangmao Wang | Hailong Cao | Weilong Zhong

Department of Gastroenterology and Hepatology, General Hospital, Tianjin Medical University, National Key Clinical Specialty, Tianjin Institute of Digestive Diseases, Tianjin Key Laboratory of Digestive Diseases, Tianjin, China

**Correspondence**
Weilong Zhong and Hailong Cao, Department of Gastroenterology and Hepatology, General Hospital, Tianjin Medical University, National Key Clinical Specialty, Tianjin Institute of Digestive Diseases, Tianjin Key Laboratory of Digestive Diseases, 154 Anshan Road, Heping District, Tianjin 300052, China.
Email: zhongweilong@tmu.edu.cn; caohailong@tmu.edu.cn

**Funding information**
National Natural Science Foundation of China, Grant/Award Number: 81970477, 82000511, 82070545, 82100574 and 82270574; Key Project of Science and Technology Pillar Program of Tianjin, Grant/Award Number: TJYXZDXK-002A and 20YFZCSY00020; Tianjin Key Medical Discipline (Specialty) Construction Project

## Abstract

Colorectal cancer (CRC) is related to gut microbiota dysbiosis, especially butyrate-producing bacteria reduction. Our previous study suggested that administration of *Clostridium butyricum*, a butyrate-producing bacterium, exerts a crucial effect against CRC, however the potential mechanism is not clear. We first found that methyltransferase-like 3 (METTL3) showed a positive correlation with proliferation, epithelial–mesenchymal transition (EMT), DNA repair, metastasis, and invasion in a database analysis. The expression of METTL3 gradually increased from human normal colon tissue, to adenoma, and carcinoma, and was positively correlated with E-cadherin and CD34 levels. Overexpression of METTL3 promoted the proliferation, migration, and invasion of CRC cells and induced vasculogenic mimicry (VM) formation. *Clostridium butyricum* could downregulate METTL3 expression in CRC cells and decrease the expression of vimentin and vascular endothelial growth factor receptor 2 to reduce EMT and VM formation. *Clostridium butyricum* alleviated the pro-oncogenic effect of METTL3 overexpressing plasmid in CRC cells. The anti-EMT effect on METTL3 reduction of *C. butyricum* could be blunted by knocking down G-protein coupled receptor 43. Moreover, *C. butyricum* prevented EMT and VM and inhibited tumor metastasis in nude mice. Accordingly, *C. butyricum* could inhibit EMT and VM formation of intestinal carcinogenesis through downregulating METTL3. These findings broaden our understanding of probiotics supplement in CRC prevention and treatment.

KEYWORDS
*Clostridium butyricum*, colorectal cancer, epithelial–mesenchymal transition, methyltransferase-like 3, vasculogenic mimicry

**Abbreviations:** CB, *Clostridium butyricum*; CRC, colorectal cancer; DCA, deoxycholic acid; EMT, epithelial–mesenchymal transition; F, forward; GO, Gene Ontology; GPR43, G-protein coupled receptor 43; IHC, immunohistochemistry; KEGG, Kyoto Encyclopedia of Genes and Genomes; m6A, N6-methyadenosine; METTL3, methyltransferase-like 3; NaBu, sodium butyrate; PAS, periodic acid–Schiff; R, reverse; SCFAs, short-chain fatty acids; SNHG10, small nucleolar RNA host gene 10; VEGFR2, vascular endothelial growth factor receptor 2; VM, vasculogenic mimicry.

Kexin Zhang, Yue Dong, Mengfan Li, and Wanru Zhang contributed equally to this work.

## 1 | INTRODUCTION

Colorectal cancer is acknowledged as a prominent cause of mortality worldwide, accompanied by common tumor metastasis or recurrence.[1] The intestinal micro-ecological system imbalance, especially gut microbiota dysbiosis, is considered one of the mechanisms of CRC progression.[2–4] Numerous studies have confirmed intestinal pathogens, such as *Fusobacterium nucleatum* and enterotoxigenic *Bacteroides fragilis*, could initiate aggressive tumor process in CRC patients.[5,6] As a butyrate-producing gut symbiont, *Clostridium butyricum* abund has been reported a remarkable reduction in patients with CRC compared with healthy individuals.[7,8] The present study suggested that the increased levels of SCFAs by *C. butyricum* administration contributed to its protective effects on CRC.[9,10] However, our previous results showed that there was no significant difference in the contents of SCFAs between the *C. butyricum* group and the heat-killed *C. butyricum* group.[11] *Clostridium butyricum* could suppress the extracellular nucleic acids and protein components of enterotoxigenic *B. fragilis* to inhibit severe intestinal cancer.[12] *Clostridium butyricum* has been proved to stimulate GPR43 and GPR109A and suppress the Wnt/β-catenin signaling pathway to ameliorate intestinal tumorigenesis.[13] It has been reported that butyrate produced by *Faecalibacterium prausnitzii* could activate GPR43 to achieve improvement in gut permeability.[14] Extensive research has revealed that intervention of CRC cells with *C. butyricum* could improve gut barrier function, induce anti-inflammatory immunity, inhibit cancer cell proliferation, and motivate apoptosis.[15–17]

N6-methyadenosine governs gene expression through posttranscriptional modulation.[18] Methyltransferase-like 3 has been identified as an m6A-dependent methyltransferase in part responsible for epigenetic alterations of oncogenes.[19,20] Survival analysis has shown that high expression of METTL3 was related to poor CRC clinical outcomes.[21–23] Methyltransferase-like 3 not only affected the prognosis of CRC patients but also antagonized the therapeutic effect of chemotherapy drugs, such as 5-fluorouracil.[24] Epithelial–mesenchymal transition induces a critical course linked to cancer metastasis.[25,26] Changes in EMT key molecules, including E-cadherin decrease and vimentin increase, have shown tumorigenic roles in CRC.[27] Methyltransferase-like 3 could promote tumor cell invasion and migration by accelerating EMT formation.[28] Malignant tumor cells can form tubular neovascularization by VM to promote cancer invasion.[29,30] Epithelial–mesenchymal transition seems to be connected with the VM process of tumor migration in prior research.[31] Emerging studies have unveiled that *F. nucleatum* affected METTL3 to modulate CRC occurrence and aggressiveness.[32,33] Nonetheless, the underlying mechanisms of gut probiotic *C. butyricum* against METTL3 carcinogenesis need further exploration.

We addressed whether *C. butyricum* could exert an inhibitory effect by downregulating METTL3 on EMT and VM against CRC. The outcomes showed that *C. butyricum* restrained intestinal tumor proliferation and migration by reducing the expression of METTL3 in vitro and in vivo. *Clostridium butyricum* accommodation on the levels of E-cadherin, vimentin, and VEGFR2 was observed to elucidate the molecular mechanism in EMT and VM formation of tumor cells. Our work highlighted the potential efficacy of *C. butyricum* intervention to target CRC probiotic therapy.

## 2 | MATERIALS AND METHODS

### 2.1 | CancerSEA analysis

CancerSea (http://biocc.hrbmu.edu.cn/cancersea/home.jsp) provides diverse functional status of cancer cells at the single-cell level in a comprehensive database. Through the website, we studied average correspondence between METTL3 proteins and cell functional states.

### 2.2 | Protein–protein interaction network analysis

STRING (https://string-db.org/) was used to analyze the protein–protein interaction network relationship of proteins interacting with METTL3. We identified interactions between forecasted and known proteins by utilizing the STRING database that is suitable for 2031 species. The STRING database contains experimental data, results mined from PubMed abstracts, integrated data from other databases, as well as predicted results from bioinformatics methods.

### 2.3 | LinkedOmics analysis

The coexpressive genes of METTL3 and their involvement in GO and KEGG enrichment analysis were analyzed by the LinkedOmics database. We registered to access LinkedOmics (http://linkedomics.org/login.php), selected filter criteria in the search interface, and downloaded the data related to the relative level and biological process of the *METTL3* gene in CRC, then statistically analyzed the expression of METTL3 in different types of single cells.

### 2.4 | Clinical sample collection

This study enrolled patients with intestinal adenoma or adenocarcinoma diagnosed by colonoscopy in the Digestive Endoscopy Center, Tianjin Medical University General Hospital. We also recruited controls from patients who underwent colonoscopy with hyperplastic polyps or no pathological changes.

### 2.5 | Bacterial preparation

*Clostridium butyricum* (ATCC 19398), provided by the China General Microbiological Culture Collection Center, was planted in brain heart infusion broth, then incubated for 24 h under a 37°C oxygen-free environment until the bacterial density was 0.5 at A600. *Clostridium butyricum* was collected by centrifugation (3000 *g* × 5 min) and resuspended to the final concentration

of $2\times10^9$ CFU/0.2 mL with sterile PBS. *Clostridium butyricum* supernatant was gathered, percolated with 0.22 μm percolators, and then deliquated with medium.

## 2.6 | Cell culture

The human CRC cell lines (HCT116, Caco-2) were acquired from ATCC. HCT116 cells were reproduced in DMEM covering 10% FBS and 1% penicillin–streptomycin solution. Caco-2 cells were incubated in minimum essential medium supplemented with 20% FBS and 1% penicillin–streptomycin solution. Both CRC cell lines were maintained in a 5% $CO_2$ incubator at 37°C constant temperature.

## 2.7 | Animal experiments

The 4-week-old female BALB/c nude mice were purchased and raised in a specific pathogen-free environment at Tianjin International Joint Academy of Biomedicine. We randomly divided 12 BALB/c nude mice into the control group and the 20% CB supernatant group. The transplanted tumor was formed by subcutaneous injection of HCT116 cells ($2\times10^6$ cells/each mouse). After approximately 5 days, the nodules could be touched subcutaneously. Subsequently, the control group mice were injected with PBS (200 μL) along the periphery of the tumor, and the experimental group mice were injected with *C. butyricum* supernatant (200 μL). The frequency of this treatment was once every other day; the long and short diameters of the tumor were measured every day, as well as the weight. When the tumor volume increased by approximately 150 $mm^3$, the mice were killed and the tumor was stripped and stored in 4% tissue fixation solution. The Institutional Animal Care and Use Committee of Tianjin Medical University authorized our animal experiments.

## 2.8 | Histological analysis and IHC

In IHC, the tissue was incubated with primary Abs as follows: anti-METTL3 (1:2000; Abcam), anti-E-cadherin (1:800; Cell Signaling Technology), anti-vimentin (1:400; Affinity), and anti-CD34 (1:100; Abcam).

## 2.9 | Real-time PCR

The cell lysates of cancer cells cultured in vitro were homogenized with TRIzol reagent (cat#15596026; Ambion). RNA was purified by the RNeasy Mini Kit (Qiagen). Complementary DNA was synthesized by RT carried out with the TIANScript RT Kit (Tiangen). The standard $2^{-\Delta\Delta Ct}$ method was adopted to measure gene in mRNA levels. Real-time PCR was used to amplify METTL3 primers (F, CAAGC TGCACTTCAGACGAA; R, GCTTGGCGTGTGGTCTTT), vimentin primers (F, GGAGAAACCTGCCAAGTATG; R, TGGGAGTTGCTGTT GAAGTC), GPR43 primers (F, CACCGAGAACCAAATCACCT; R, GTCATGGGGACGAAAAAGAG), and GAPDH primers (F, GGAGA AACCTGCCAAGTATG; R, TGGGAGTTGCTGTTGAAGTC).

## 2.10 | Western blot analysis

We used RIPA buffer (Solarbio) to extract the total cell protein. The following appropriate primary Abs were incubated at 4°C overnight, including anti-METTL3 (1:1000; Abcam), anti-VEGFR2 (1:1000; Abcam), anti-E-cadherin (1:1000; Cell Signaling Technology), anti-vimentin (1:1000; Affinity), anti-GAPDH (1:3000; Affinity), and anti-β-actin (1:1000; Cell Signaling Technology). The protein bands were visualized by enhanced chemiluminescence and quantified by densitometry using ImageJ software (NIH).

## 2.11 | Cell proliferation assay

HCT116 and Caco-2 cells were inoculated into 96-well plates. Each group was offered five parallel holes (2000 cells per hole). Cell viability was measured after treatment with METTL3 plasmid or 5%, 10%, or 20% CB supernatant for 0, 12, 24, and 48 h using CCK-8 (Beyotime). The CCK-8 reagent was mixed in one well apiece in every test point. After 1 h at 37°C, a microplate reader was used at the wavelength of 450 nm to measure the absorbance.

## 2.12 | Three-dimensional culture

The formation of angiogenesis simulation was gauged by 3D culture containing Matrigel. We applied 50 μL Matrigel to the 24-hole plate and solidified it for 1 h at 37°C. HCT116 and Caco-2 cells were treated with 20 μM METTL3 overexpressed plasmid then inoculated at a concentration of $5\times10^5$ on a plate that was covered with coagulation matrix. We took advantage of the inverted microscope to obtain tube-like structures after 6 h, and then quantified and analyzed the number of complete VM structures.

## 2.13 | Wound healing assay

We incubated HCT116 or Caco-2 cells in 48-well boards overnight to form uniform monolayers, accounting for at least 90% of the plates. We used the tip of a 200 μL pipette to produce scratches. Methyltransferase-like 3 overexpressing plasmid or METTL3 overexpressing plasmid with 20% CB supernatant was used to treat cells for 1 day. Every group was repeated in four or five parallel holes. After scratching, we applied an inverted microscope (magnification 40×) to capture wound closure in a consistent position at 0, 12, 24, and 48 h or 0, 5, and 10 h separately. The wound area of cells was measured by ImageJ.

### 2.14 | Overexpression of METTL3

We treated HCT116 cells and Caco-2 cells with METTL3 overexpressing plasmid (Obio Technology) and Lipofectamine 2000 (Invitrogen). The transfection concentration was 0.4 μg for HCT116 cells and 0.8 μg for Caco-2 cells. After transfection of plasmid for 4 h, we replaced it with culture medium or 20% CB supernatant.

### 2.15 | Knockdown of GPR43 using siRNA

Gene silencing of GPR43 was carried out in HCT116 cells as described previously.[13] We transfected with siRNA targeting GPR43 (GenePharma). GPR43 siRNA or control siRNA (0.5 μg per well) was incubated in HCT116 cells transiently by Lipofectamine 2000 (Invitrogen) in Opti-MEM (Gibco). After 5 h, DMEM or 20% CB supernatant was used to refresh HCT116 cells for 24 h.

### 2.16 | Statistical analysis

For statistical analysis, we used GraphPad Prism 7 software (GraphPad Software, Inc.) and presented the measurement data as mean ± SD. Then we used an independent samples *t*-test for two-group comparison. One-way ANOVA was used for different-group multiple comparisons. A *p* value of less than 0.05 was considered statistically significant.

## 3 | RESULTS

### 3.1 | Overexpression of METTL3 associated with tumor malignancy

We analyzed the average association of METTL3 with different cancer functional states using the CancerSEA database. The analytic results revealed that METTL3 level showed a positive correlation with tumor proliferation, EMT, DNA repair, metastasis, invasion, and stemness (Figure 1A,B). In addition, to more accurately describe the expression of METTL3 in different cell subtypes, we carried out high-dimensional flow cytometry analysis of each cell population of tumor tissues using the unified manifold approximation and projection (UMAP) dimensionality reduction method. The results showed that METTL3 might be highly expressed, especially in distal enterocytes as well as undifferentiated cells (Figure 1C). Moreover, we explored the scatter of METTL3 abundance of all single cells using the t-SNE plot, where the color depth correlated with METTL3 level. Our results indicated that cells with less METTL3 abundance obviously clustered, as did cells with higher METTL3 abundance (Figure 1D).

### 3.2 | METTL3 coexpressed genes affected tumor function

Furthermore, we used the public database from LinkedOmics to analyze the expression of *METTL3* coexpressed genes and related biological events (Figure 2A). The heatmaps showed genes positively and

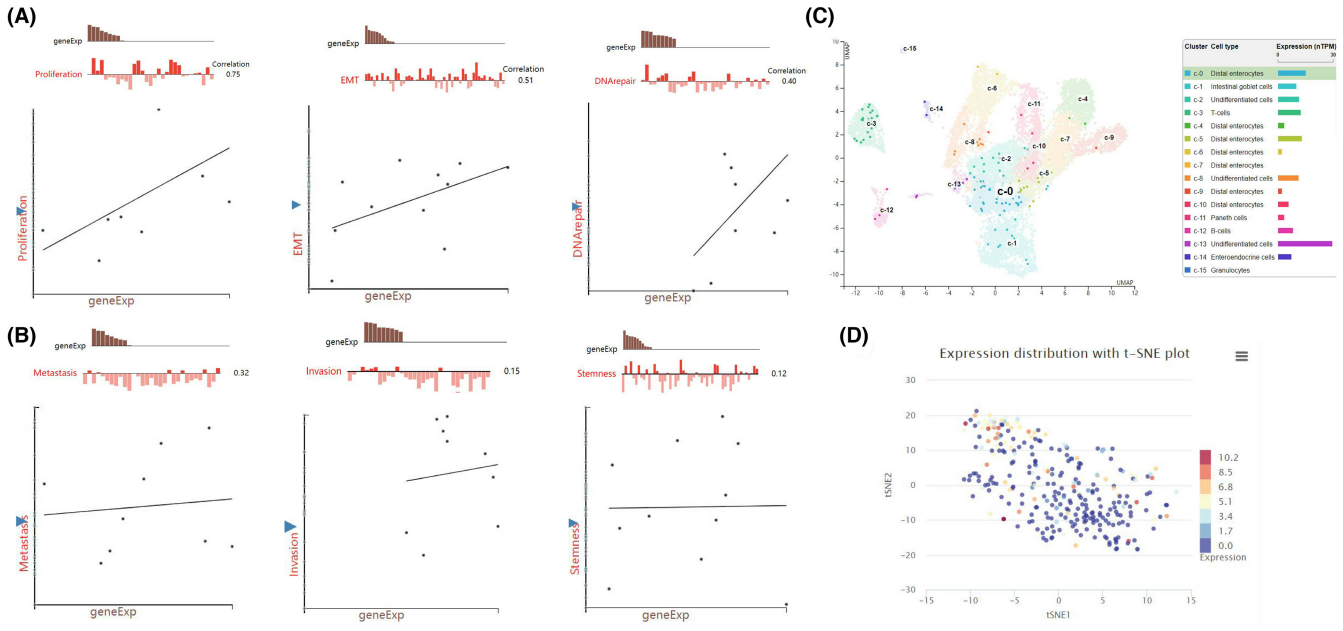


FIGURE 1 Expression of methyltransferase-like 3 (METTL3) was positively correlated with colorectal tumor malignancy. (A) Average correlation between METTL3 and functional status of colorectal cancer (CRC). The results of the analysis showed that the expression level of METTL3 was positively correlated with proliferation, epithelial–mesenchymal transition (EMT), and DNA repair. (B) The expression level of METTL3 was positively correlated with metastasis, invasion, and stemness. (C) Unified manifold approximation and projection (UMAP) plot indicated the relationship between different cell groups and METTL3 expression. (D) The scatter of METTL3 expression in CRC and the t-SNE plot of all individual cells.

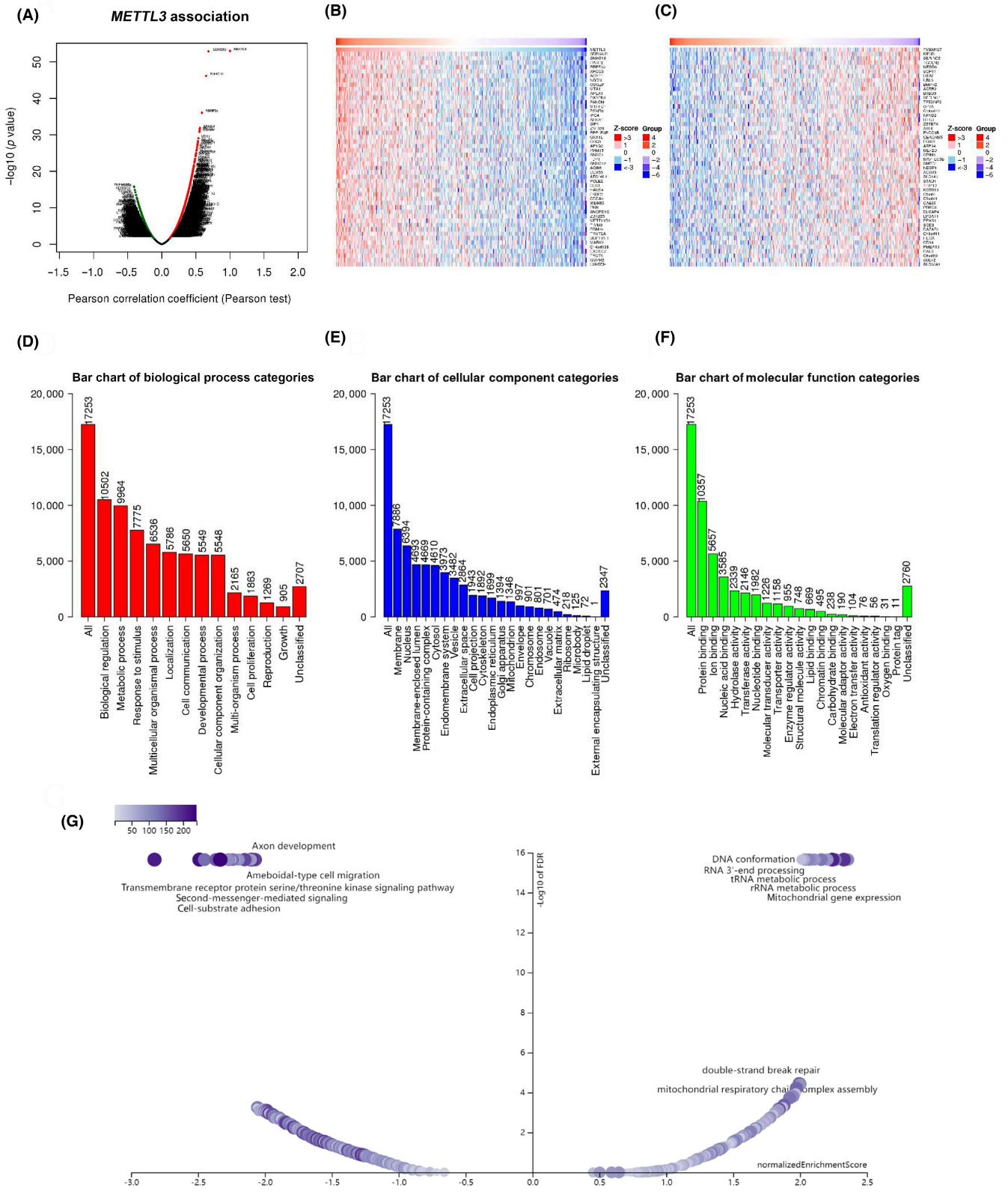


FIGURE 2 *METTL3* coexpressed genes affected the function of tumor. (A) Volcano map analysis results of *METTL3* coexpressed genes. (B) Heatmap analysis of coexpressed genes positively correlated with *METTL3*. Red indicates positive genes; green indicates negative genes. (C) Heatmap analysis of negatively correlated genes coexpressed with *METTL3*. Red indicates positive genes; green indicates negative genes. (D) Biological process enrichment analysis of *METTL3* coexpressed genes. (E) Cellular component enrichment analysis of *METTL3* coexpressed genes. (F) Molecular function enrichment analysis of *METTL3* coexpressed genes. (G) Kyoto Encyclopedia of Genes and Genomes enrichment analysis of *METTL3* coexpressed genes.

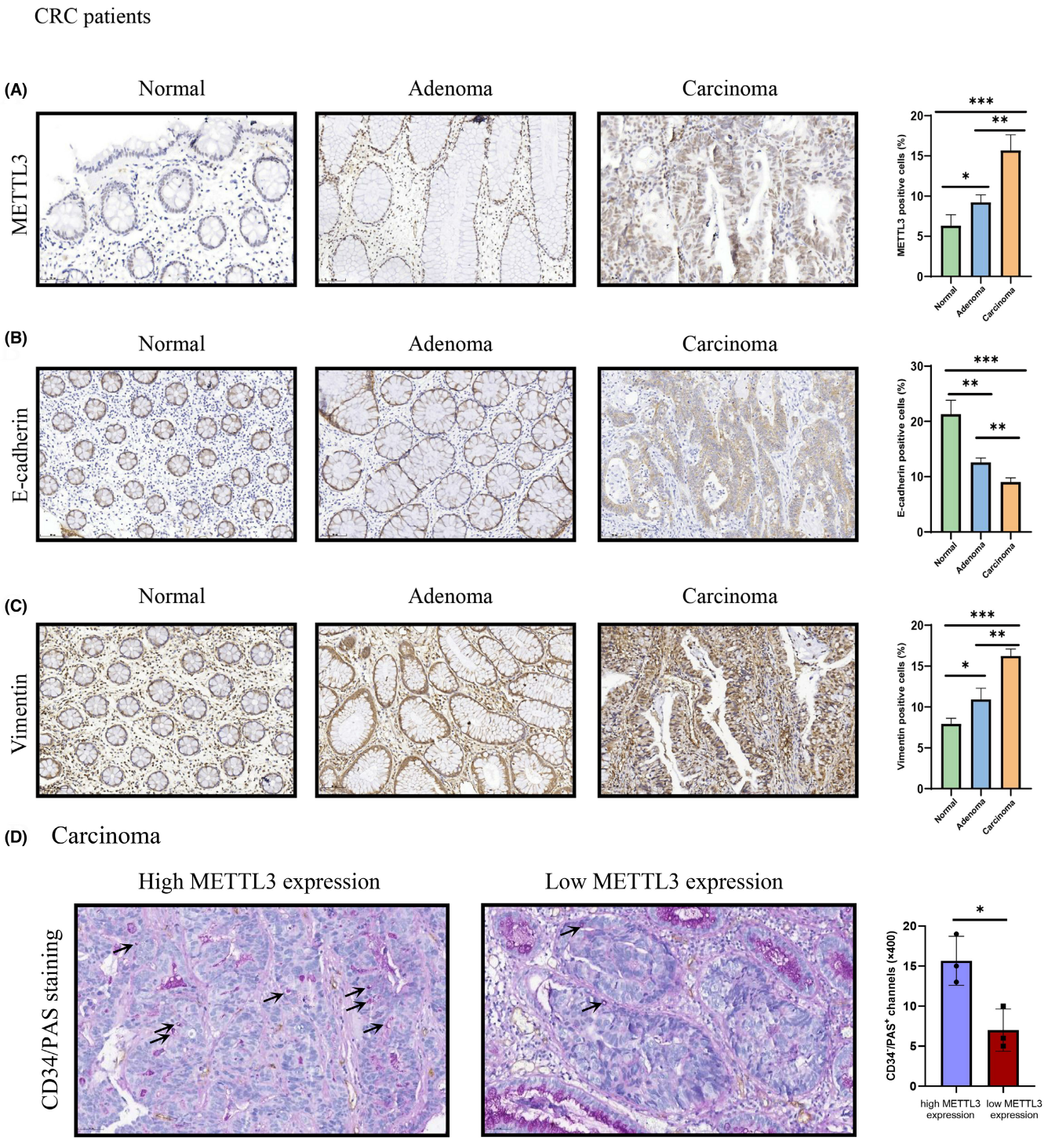


**FIGURE 3** Development of epithelial–mesenchymal transition and vasculogenic mimicry (VM) along with increased methyltransferase-like 3 (METTL3) level in human colonic tissues. (A) Immunohistochemical (IHC) staining for METTL3 and the number of METTL3 positive cells in human normal colonic tissue, adenoma, and carcinoma specimens. (B) IHC staining for E-cadherin and the number of E-cadherin positive cells in human normal colonic tissue, adenoma, and carcinoma specimens. (C) IHC staining for vimentin and the number of vimentin-positive cells in human normal colonic tissue, adenoma, and carcinoma specimens. (D) CD34/periodic acid–Schiff (PAS) double staining displayed VM channels in human colorectal cancer specimens with high and low expression of METTL3. Scale bar, 50 μm. $^{*}p<0.05$, $^{**}p<0.01$, $^{***}p<0.001$.

**FIGURE 4** Overexpressed methyltransferase-like 3 (METTL3) facilitated colorectal cancer cell proliferation, migration, and invasion, which could be inhibited by *Clostridium butyricum* (CB). (A) Effect of METTL3 overexpression on the proliferation ability of HCT116 and Caco-2 cells. (B) Effect of METTL3 overexpression on cell migration ability was analyzed by scratch test in HCT116 and Caco-2 cells. (C) Effects of METTL3 overexpression on proliferation ability were analyzed by CCK-8 in HCT116 and Caco-2 cells. (D) Relative expressions of METLL3 in HCT116 and Caco-2 cells were detected by real-time PCR. (E) Protein levels of METTL3 in HCT116 cells were analyzed by western blotting using anti-β-actin as internal control (Con). Scale bar, 100 μm. $^{*}p<0.05$, $^{**}p<0.01$, $^{***}p<0.001$. NaBu, sodium butyrate.

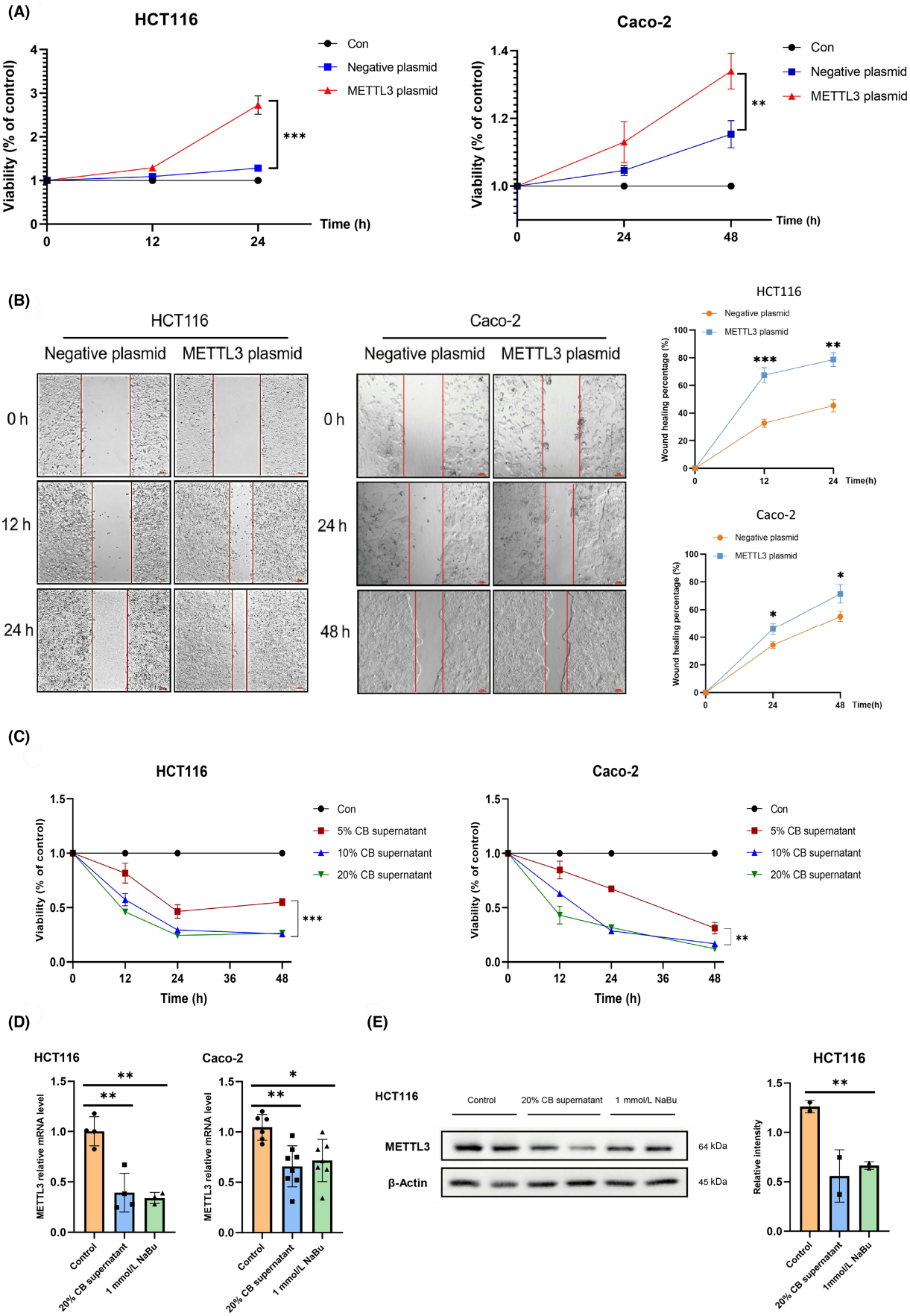
(A)
HCT116
Viability (% of control)
Time (h)
Con
Negative plasmid
METTL3 plasmid
***
Caco-2
**
(B)
HCT116
Caco-2
Negative plasmid
METTL3 plasmid
0 h
12 h
24 h
48 h
Wound healing percentage (%)
Time(h)
(C)
HCT116
Caco-2
Con
5% CB supernatant
10% CB supernatant
20% CB supernatant
Viability (% of control)
Time (h)
(D)
METTL3 relative mRNA level
Control
20% CB supernatant
1 mmol/L NaBu
(E)
HCT116
Control
20% CB supernatant
1 mmol/L NaBu
METTL3
β-Actin
64 kDa
45 kDa
Relative intensity

negatively associated with *METTL3* (Figure 2B,C). The analysis revealed that *METTL3* coexpression was positively correlated with *SNHG10* and negatively correlated with *TMEM127* and *KIF3B*. These findings indicated that *METTL3* coexpressed genes might result in tumor development by protein interaction. In addition, we utilized GO and KEGG analyses to concentrate on METTL3-related biological processes. Related molecular functions chiefly covered protein, ion, and nucleic acid binding (Figure 2D–F). Additionally, the pathways affected by METTL3 covered ameboidal-type cell migration, cell-substrate adhesion, DNA conformation, and double-strand break repair (Figure 2G).

### 3.3 | Development of EMT and VM correlated with increased METTL3 level in human colonic tissues

To determine the relevancy of METTL3 and CRC evolvement, we detected METTL3 expression and the related parameters of EMT and VM in human colonic tissues. We found that METTL3 level increased incrementally from human normal colonic tissue to adenoma to carcinoma (Figure 3A). Moreover, IHC showed a tendency of reduced E-cadherin expression and rising vimentin expression in these three tissues, with statistical significance (Figure 3B,C). E-cadherin and vimentin served as epithelial parameters and mesenchymal parameters, respectively. In addition, CD34/PAS double staining showed that the VM-positive channel was apparently higher in carcinoma tissues with high expression of METTL3 compared to the carcinoma tissues with low expression of METTL3 (Figure 3D). These results indicated that high METTL3 level could be relevant to VM formation and the EMT process in CRC.

### 3.4 | Overexpressed METTL3 facilitated CRC cell proliferation, migration, and invasion, which could be inhibited by *C. butyricum*

We further detected cell proliferation ability to better comprehend the influence of METTL3 during CRC evolvement. Our results showed that the proliferation of HCT116 and Caco-2 cells was significantly increased with the overexpression of METTL3 (Figure 4A). The scratch test confirmed that HCT116 cells treated with METTL3 plasmid had a higher migration ability in 24 h compared with the control group. Caco-2 cells with METTL3 also had a higher migration ability in 48 h. Our findings indicated METTL3 induced tumor cell proliferation, migration, and invasion (Figure 4B). The 20% CB supernatant strongly minimized HCT116 cell viability, in a time-dependent manner. The experiment with Caco-2 cells revealed the same pattern (Figure 4C). Furthermore, we observed a decreased relative mRNA level of METTL3 by real-time PCR in the 20% CB supernatant group and 1 mmol/L sodium butyrate (NaBu) group, which was a positive control (Figure 4D). Western blot analysis also illustrated the decreased protein expression of METTL3 in the 20% CB supernatant group and 1 mmol/L NaBu group (Figure 4E). The results offered evidence of similar effects of CB supernatant and NaBu on METTL3 inhibition. Thus, it can be concluded METTL3 overexpression motivates CRC cell proliferation, migration, and invasive abilities, which might be a critical correlation with *C. butyricum*.

### 3.5 | *Clostridium butyricum* inhibited EMT and VM formation in CRC cells

We used western blot analysis to explore the influence of CB supernatant on METTL3-mediated EMT and VM of HCT116 cells. *Clostridium butyricum* supernatant reduced the expression of VEGFR2 and vimentin and elevated the E-cadherin expression induced by METTL3 overexpression, emphasizing the vital influence of *C. butyricum* on METTL3-mediated EMT and VM processes (Figure 5A). Scratch test suggested that after METTL3 overexpression, the displacement rate of HCT116 cells was higher and the wound area was narrower, reflecting that overexpression of METTL3 accelerated migration in HCT116 cells. However, CB supernatant significantly inhibited the above effects of METTL3 (Figure 5B). Cell tubule formation experiments confirmed that the ability to form vessel-like tubes in HCT116 cells was enhanced due to overexpressing METTL3. After CB supernatant treatment, the number of cell tubules induced by overexpression of METTL3 decreased (Figure 5C). Taken together, CB supernatant inhibited the effect of overexpressed METTL3 on promoting EMT and VM formation of HCT116 cells, thus reducing the invasiveness of cancer cells.

### 3.6 | *Clostridium butyricum* suppressed tumor development and metastasis in nude mice xenograft model

To investigate the role of *C. butyricum* in relieving malignant progression in vivo, the subcutaneous region of mice was constructed by injecting HCT116 cells to establish a xenograft model (Figure 6A). Xenograft tumor model weight increased more drastically in the control group, compared with the 20% CB supernatant group (Figure 6B). The CB-treated nude mice had smaller tumor volume and slower tumor growth, which showed the antineoplastic effect of CB supernatant (Figure 6C,D). We identified METTL3, EMT biomarkers, and

**FIGURE 5** *Clostridium butyricum* (CB) inhibits epithelial–mesenchymal transition and vasculogenic mimicry formation in colorectal cancer cells. (A) Western blot analysis after *C. butyricum* treatment showing expression levels of vascular endothelial growth factor receptor 2 (VEGFR2), vimentin, and E-cadherin proteins in HCT-116 cells overexpressed with methyltransferase-like 3 (METTL3). (B) Scratch test showing that *C. butyricum* inhibited migration induced by METTL3 in HCT-116 cells. Quantitative measurement results of wound closure in four groups were analyzed. (C) Three-dimensional culture showing images of vessel-like tubular structures (arrows). Numbers of corresponding patterned networks were counted under an inverted microscope. Scale bar, 100 μm. $^{*}p < 0.05$, $^{**}p < 0.01$, $^{***}p < 0.001$.

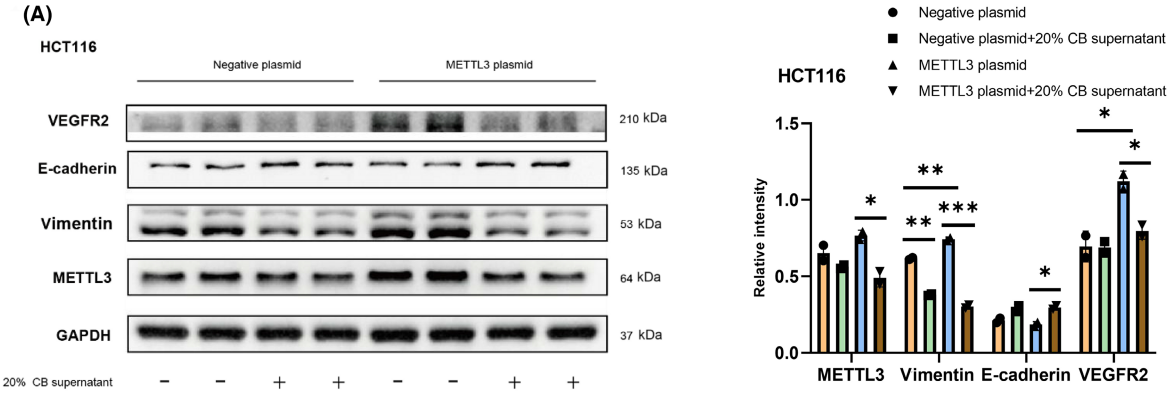
(A)
HCT116
Negative plasmid
METTL3 plasmid
VEGFR2
E-cadherin
Vimentin
METTL3
GAPDH
210 kDa
135 kDa
53 kDa
64 kDa
37 kDa
20% CB supernatant
Negative plasmid
Negative plasmid+20% CB supernatant
METTL3 plasmid
METTL3 plasmid+20% CB supernatant
HCT116
Relative intensity
METTL3
Vimentin
E-cadherin
VEGFR2

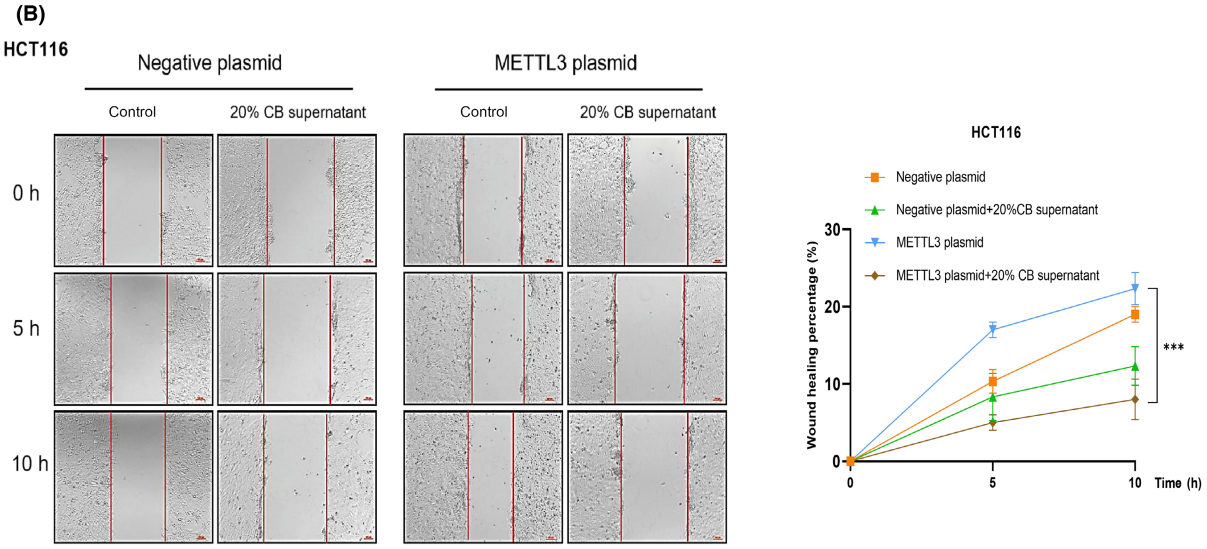
(B)
HCT116
Negative plasmid
METTL3 plasmid
Control
20% CB supernatant
0 h
5 h
10 h
HCT116
Negative plasmid
Negative plasmid+20%CB supernatant
METTL3 plasmid
METTL3 plasmid+20% CB supernatant
Wound healing percentage (%)
Time (h)

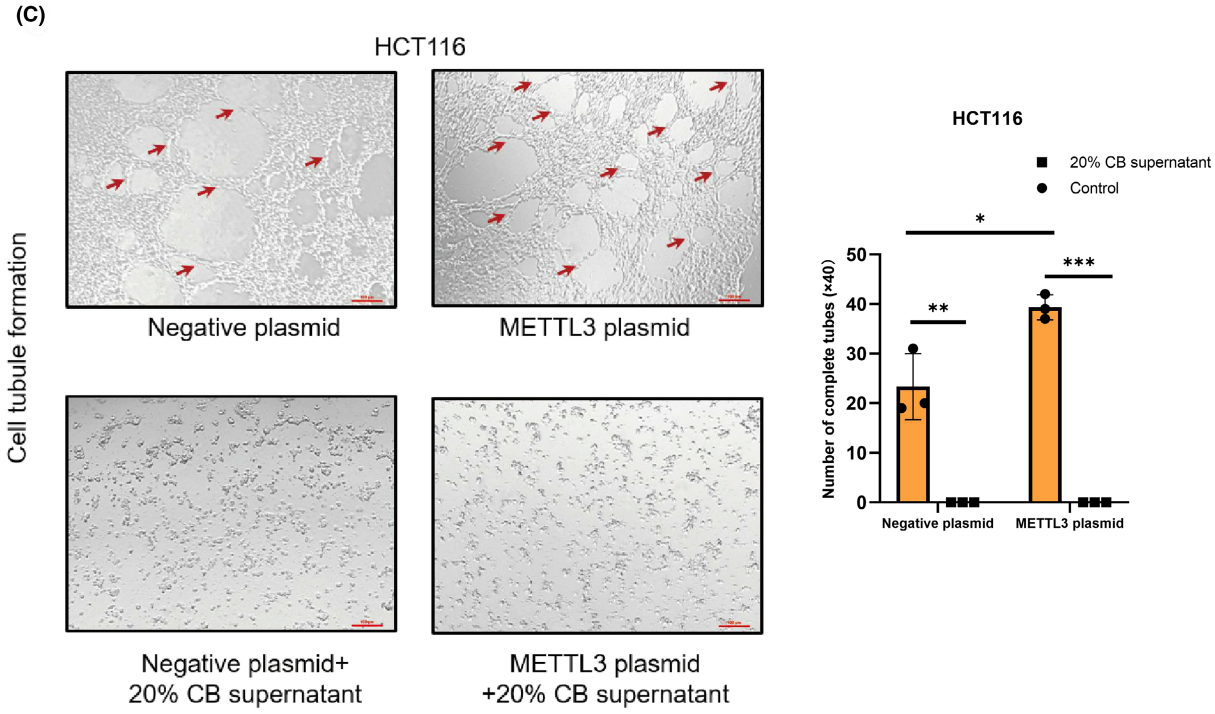
(C)
HCT116
Cell tubule formation
Negative plasmid
METTL3 plasmid
Negative plasmid+
20% CB supernatant
METTL3 plasmid
+20% CB supernatant
HCT116
20% CB supernatant
Control
Number of complete tubes (×40)
Negative plasmid
METTL3 plasmid

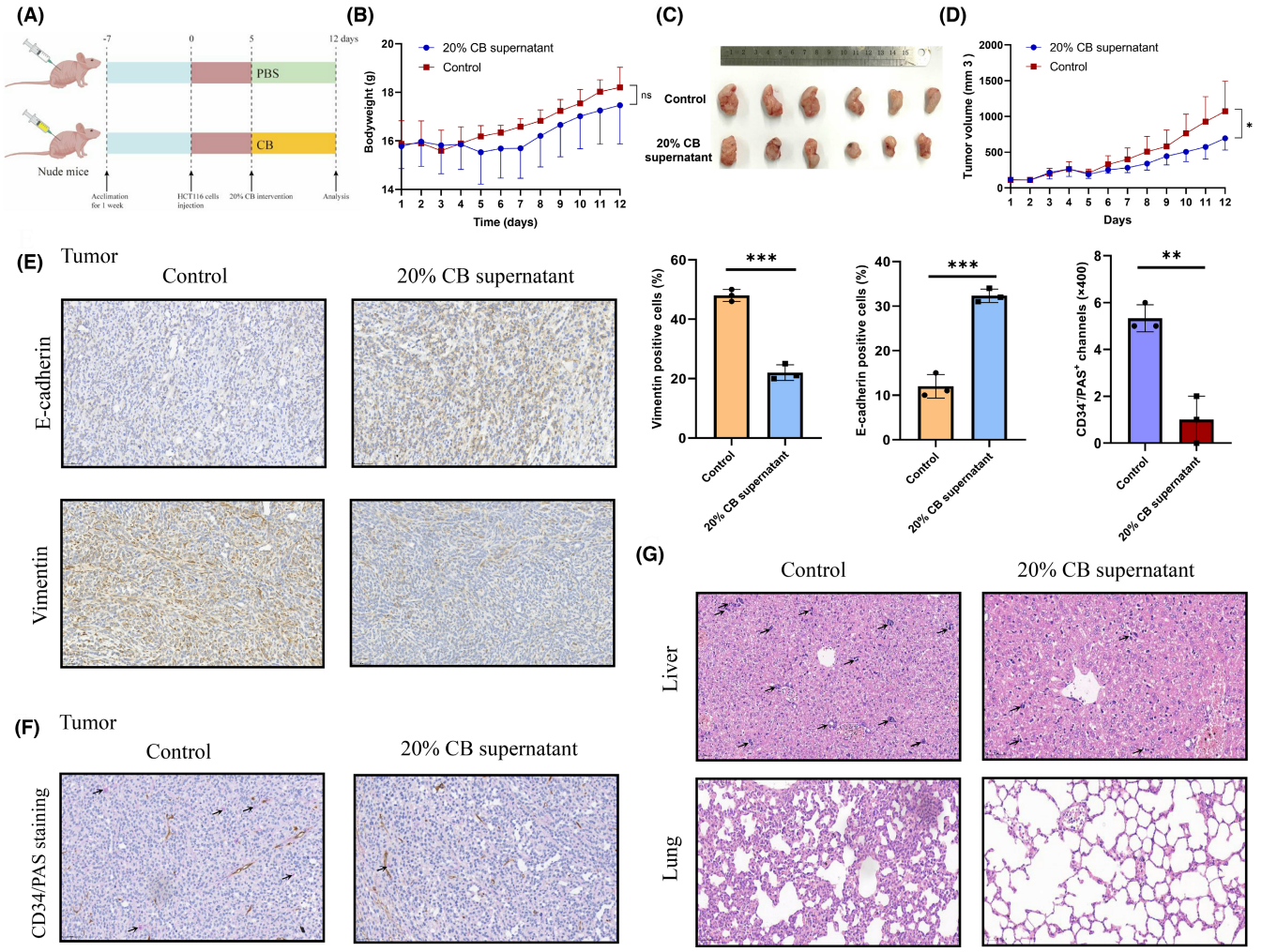


FIGURE 6 *Clostridium butyricum* (CB) suppressed tumor development and metastasis in a nude mouse xenograft model. (A) HCT116 cells were transplanted on nude mice. (B) Nude mouse xenograft model showing bodyweight in the control and 20% CB supernatant groups. (C) Tumor volumes were measured every day. (D) Gross tumors from nude mice. (E) Immunohistochemical staining indices of methyltransferase-like 3 (METTL3), E-cadherin, and vimentin. (F) CD34/periodic acid–Schiff (PAS) staining was detected to assess vasculogenic mimicry formation. (G) Nude mouse xenograft model of the colorectal cancer (CRC) cell line HCT116 showed that *C. butyricum* suppressed liver and lung metastasis of CRC. Each experiment was repeated at least three times. Scale bar, 50 μm. $^{*}p<0.05$, $^{**}p<0.01$, $^{***}p<0.001$.

VM-related proteins in the control and 20% CB supernatant groups by IHC staining. *Clostridium butyricum* treatment displayed reduced METTL3 with depleted vimentin protein and strong E-cadherin staining (Figure 6E). Identically, CD34/PAS staining was identified to show less tube formation in the 20% CB supernatant group (Figure 6F). Staining with H&E in liver and lung tissues to assess the effect of CB supernatant on the metastasis in vivo. In contrast to the control group, the 20% CB supernatant supplement significantly reduced the metastasis of HCT116 cells to the liver and lung (Figure 6G).

### 3.7 | *Clostridium butyricum* inhibited METTL3 and EMT process by upregulating GPR43

Our previous data showed that CB supernatant-produced butyrate could bind to GPR43 with close affinity to suppress CRC cell proliferation and induce apoptosis.[13] *Clostridium butyricum* may downregulate METTL3 and EMT through GPR43 and we used the siRNA that targets GPR43 to silence the *GPR43* gene to verify results. As expected, *C. butyricum* promoted GPR43 activation and marked GPR43 mRNA reduction was observed under GPR43 siRNA transfection (Figure 7A). After GPR43 knockdown, there was no significant difference in METTL3 mRNA level, with or without 20% CB supernatant (Figure 7B). The level of vimentin, a key target of EMT progression, was decreased under the condition of *C. butyricum* intervention and GPR43 silencing limited the *C. butyricum* anti-EMT effect (Figure 7C). Similarly, due to GPR43 siRNA transfection, the favorable results of 20% CB supernatant on E-cadherin, vimentin, and METLL3 protein expressions were blocked (Figure 7D). In summary, depletion of GPR43 blunted *C. butyricum*-induced METTL3 reduction and EMT inhibition.

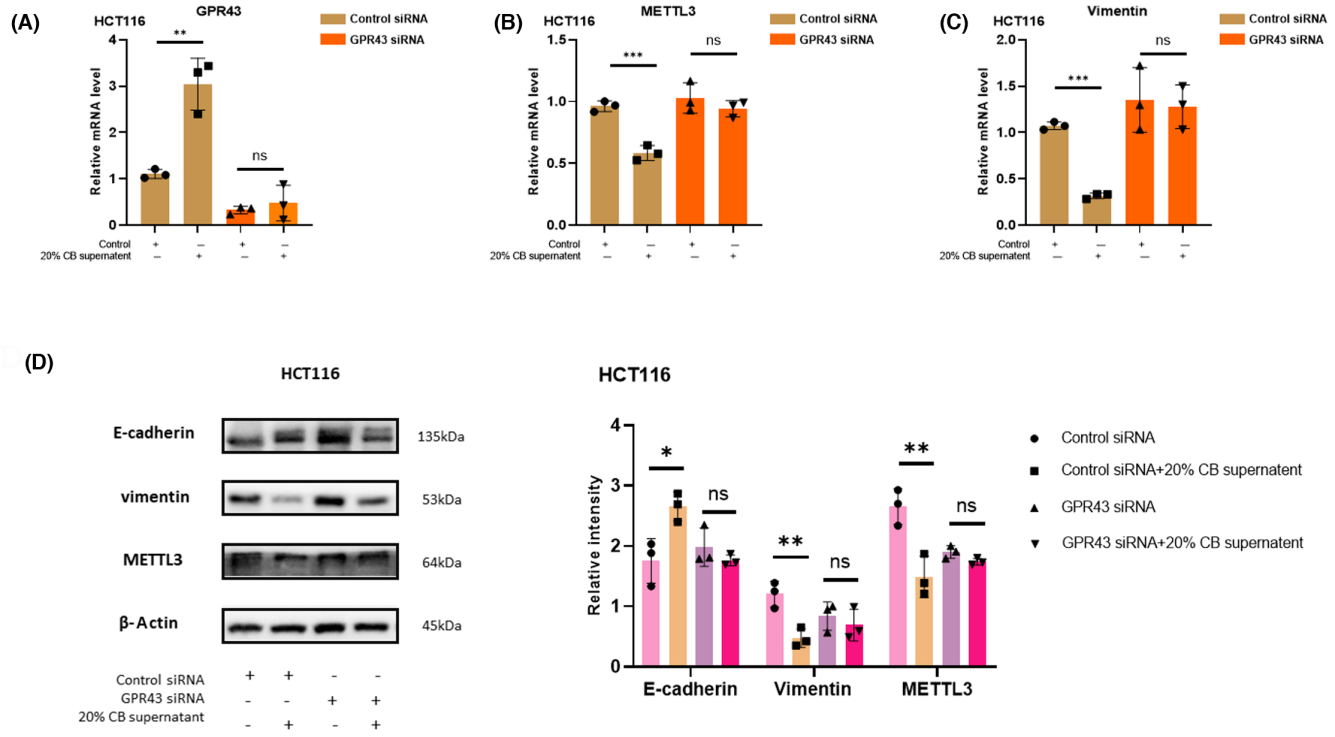


FIGURE 7 *Clostridium butyricum* (CB) inhibited methyltransferase-like 3 (METTL3) and epithelial–mesenchymal transition by upregulating G-protein coupled receptor 43 (GPR43). (A) Knockdown transfection effect and *C. butyricum* treatment of GPR43 siRNA and control siRNA is shown by real-time PCR in HCT116 cells. (B) mRNA expression of METTL3 under the condition of 20% CB supernatant after GPR43 silencing. (C) mRNA level of vimentin in different treatment groups. (D) Western blot analysis showing expression levels of METTL3, vimentin, and E-cadherin proteins with or without 20% CB supernatant after GPR43 knockdown. $^{*}p<0.05$, $^{**}p<0.01$, $^{***}p<0.001$. ns, not significant.

## 4 | DISCUSSION

The finding of our study was that METTL3 gradually increased with the progression of CRC, in agreement with previous studies.[34,35] We revealed that a high METTL3 level might promote the development of CRC through EMT and VM, and overexpression of METTL3 in vitro confirmed this view. Notably, cell experiment and nude mouse model results showed that *C. butyricum* could inhibit the above-mentioned effects of METTL3 and retard the progress of CRC (Figure 8).

Methyltransferase-like 3 could motivate BHLHE41 to induce CXCL1 transcription of CRC cells and eventually accelerate myeloid-derived suppressor cell migration.[36] The knockout of METTL3 in vitro significantly inhibited tumor proliferation, migration, metastasis, and invasion.[37] A current study confirmed that the high expression of METTL3 in tumor-infiltrating myeloid cells was linked to the poor prognosis of CRC patients, which was potently induced through H3K18 lactylation.[38] As our bioinformatics analysis outcomes suggested that *METTL3* was positively coexpressed with *SNHG10*, we surmised that *SNHG10* might interact with *METTL3* to promote the EMT process. RNA sequencing suggested SNHG10 upregulated expression in EMT-derived exosomes.[39,40] Zhang et al. found that METTL3 maintained VEGFA RNA stability to promote angiogenesis in CRC in vitro.[41] Methyltransferase-like 3 upregulated PLAU mRNA through m6A modification, and regulated the MAPK/ERK pathway to promote angiogenesis and invasion in CRC.[42] Overexpression of METTL3 led to upregulation of proliferative CRC cells to promote further migration. Recent research showed that METTL3-induced CRC metastasis could be weakened by circ_0000390, which downregulated Notch1 overexpression.[43]

Epithelial–mesenchymal transition describes a reversible course in which epithelium forfeits its original characteristics and acquires the motile and invasive characteristics of mesenchymal cells.[44–46] During EMT, increased mesenchymal properties such as vimentin and reciprocal low epithelial marker levels, such as E-cadherin and occludin, induce profound alteration in loss of epithelial apical-basal polarity and enhanced cell migration.[47,48] In addition, a previous study has elucidated that EMT is closely associated with VM in cancer tissues, as manifested by high vimentin level and deficiency in E-cadherin expression in the VM-positive group, speculating that EMT-acquired cells are more prone to form VM-like vascular channels.[31] Both EMT and VM have been developed as novel therapeutic targets for CRC.

We previously found that gene knockdown with GPR43 siRNA completely or partly blunted the antiproliferative effect of *C. butyricum*, strengthening the involvement of GPR43 in *C. butyricum* in the inhibition of CRC.[13] *Clostridium butyricum* treatment decreased METLL3 expression and suspended the EMT process

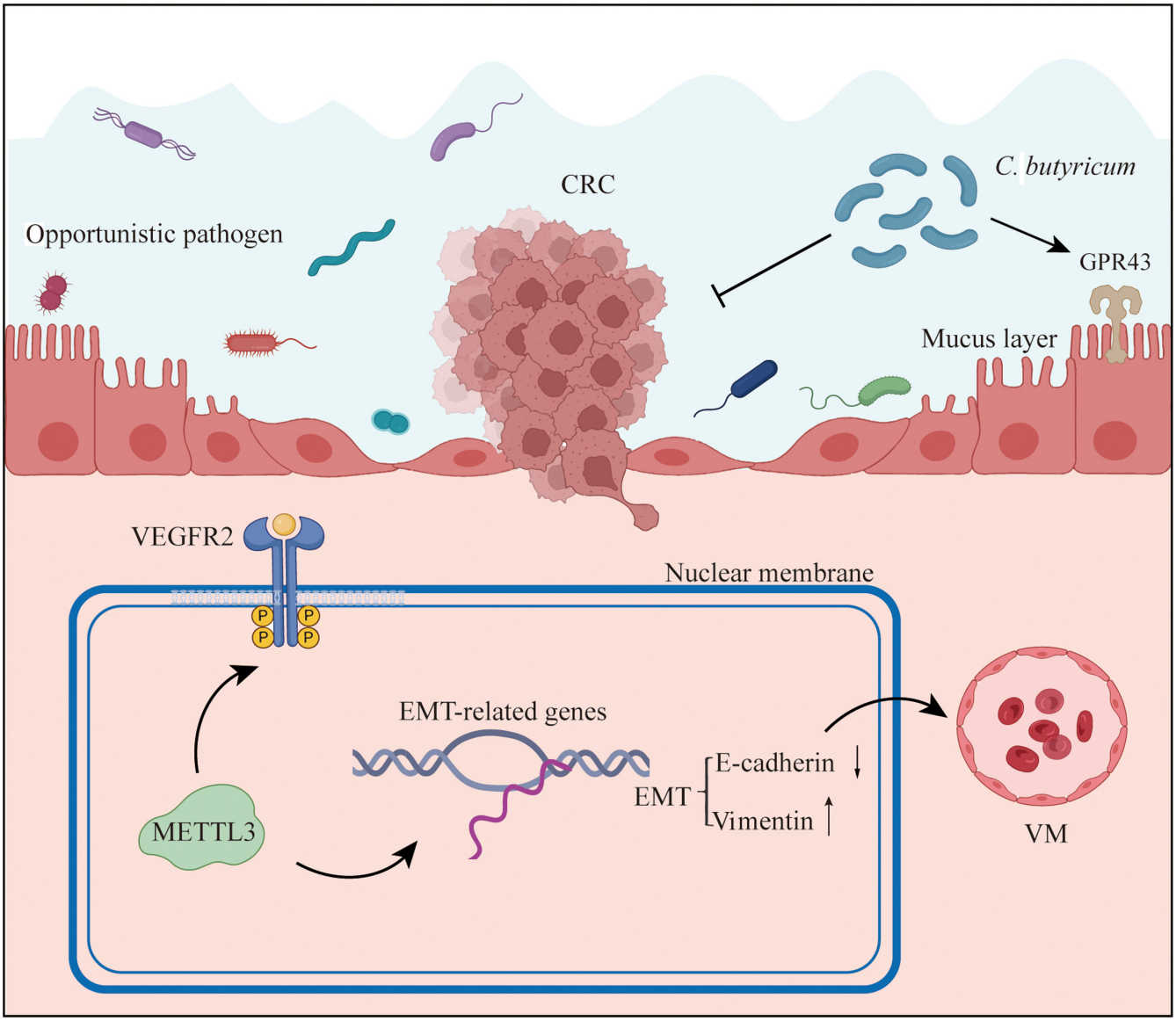


**FIGURE 8** *Clostridium butyricum* inhibits epithelial–mesenchymal transition (EMT) and vasculogenic mimicry (VM) by reducing methyltransferase-like 3 (METTL3) levels. Overexpression of METTL3 in colorectal cancer (CRC) cells leads to upregulation of vascular endothelial growth factor receptor 2 (VEGFR2) on the nuclear membrane surface. Meanwhile, METTL3 activates EMT-related genes, resulting in the synthesis of RNA and protein of downstream products E-cadherin and vimentin, and finally promotes VM. *Clostridium butyricum* can downregulate the expression of METTL3 in CRC cells, reducing the occurrence of the above events, and thus inhibiting tumor progression. *Clostridium butyricum* could activate G-protein coupled receptor 43 (GPR43) and inhibit METTL3 expression and the EMT process.

through interacting with GPR43 in our data. From experiments in vitro, we showed that *C. butyricum* slowed the growth and promoted apoptosis of CRC cells with a decreased METTL3 level and NaBu simultaneously showed the same effect. Moreover, a prior report illustrated that NaBu enabled the induction of Trx-1 protein expression downregulation, thus leading to intestinal tumor cell apoptosis and EMT retardation in CRC cells.[49] Hence, we presume that *C. butyricum* exerts the same effect consistent with NaBu and can also inhibit the formation of EMT and VM. *Fusobacterium nucleatum* was reported to promote METTL3-mediated microRNA-4717-3p maturation.[50] Supporting evidence from research showed the pro-EMT activity of *F. nucleatum* in CRC cell lines.[51–53] Zheng et al.[54] reported that adverse *F. nucleatum* overpopulation in patients and mice suppressed the beneficial *C. butyricum* population. Furthermore, Zong et al.[55] revealed that enterotoxigenic *Escherichia coli* infection can promote enteric defensin expression through the FOXO6-METTL3-m$^6$A-GPR161 signaling axis. Our previous studies have proved that DCA can promote EMT and VM through VEGFR2 activation,[31] while *C. butyricum* can reduce DCA concentration in fecal content.[13,56] Therefore, we speculate that *C. butyricum* could inhibit EMT and VM by reducing DCA.

As shown in our outcomes, *C. butyricum* treatment reduced METTL3 levels to disturb EMT and VM, indicating that *C. butyricum* inhibited CRC occurrence, invasion, and metastasis. Thus, *C. butyricum* could become a hopeful therapeutic outlook for CRC prevention and treatment. More in-depth studies are needed in this field.

## ACKNOWLEDGEMENTS

This work was supported by the National Natural Science Foundation of China (82070545, 81970477, 82000511, 82270574, and 82100574), the Key Project of Science and Technology Pillar Program of Tianjin (20YFZCSY00020), and the Tianjin Key Medical Discipline (Specialty) Construction Project (TJYXZDXK-002A).

## CONFLICT OF INTEREST STATEMENT

The authors have no conflict of interest.

## ETHICS STATEMENTS

Approval of the research protocol by an institutional review board: The study was approved by the ethics committee of Tianjin Medical University General Hospital (NO. IRB2015-YX-009).

Informed consent: Involved patients offered sufficient informed consent.

Registry and registration no. of the study/trial: N/A.

Animal Studies: All the animal care and experimental procedures were performed in accordance with the guidelines of the Institutional Animal Care and Use Committee, and the protocols were approved by the Animal Ethical and Welfare Committee of Tianjin Medical University.

## ORCID

*Hailong Cao* https://orcid.org/0000-0002-0147-7826

## REFERENCES

1. Ciardiello F, Ciardiello D, Martini G, Napolitano S, Tabernero J, Cervantes A. Clinical management of metastatic colorectal cancer in the era of precision medicine. *CA Cancer J Clin*. 2022;72:372-401.
2. Nguyen B, Fong C, Luthra A, et al. Genomic characterization of metastatic patterns from prospective clinical sequencing of 25,000 patients. *Cell*. 2022;185:563-575.e511.
3. Gatenbee C, Baker A, Schenck R, et al. Immunosuppressive niche engineering at the onset of human colorectal cancer. *Nat Commun*. 2022;13:1798.
4. Forbes N. Endoscopist adenoma detection rates and their correlation with Postcolonoscopy colorectal cancer. *Gastroenterology*. 2022;163:1714-1715.
5. Cheng Y, Ling Z, Li L. The intestinal microbiota and colorectal cancer. *Front Immunol*. 2020;11:615056.
6. Wong S, Yu J. Gut microbiota in colorectal cancer: mechanisms of action and clinical applications. *Nat Rev Gastroenterol Hepatol*. 2019;16:690-704.
7. Cani P. Gut cell metabolism shapes the microbiome. *Science*. 2017;357:548-549.
8. Ma L, Shen Q, Lyu W, et al. *Clostridium butyricum* and its derived extracellular vesicles modulate gut homeostasis and ameliorate acute experimental colitis. *Microbiol Spectr*. 2022;10:e0136822.
9. Zheng D, Li R, An J, et al. Prebiotics-encapsulated probiotic spores regulate gut microbiota and suppress colon cancer. *Adv Mater*. 2022;32:e2004529.
10. Stoeva M, Garcia-So J, Justice N, et al. Butyrate-producing human gut symbiont, clostridium butyricum, and its role in health and disease. *Gut Microbes*. 2021;13:1-28.
11. Wu J, Zhou B, Pang X, et al. *Clostridium butyricum*, a butyrate-producing potential probiotic, alleviates experimental colitis through epidermal growth factor receptor activation. *Food Funct*. 2022;13:7046-7061.
12. Shin D, Rhee K, Eom Y. Effect of probiotic clostridium butyricum NCTC 7423 supernatant on biofilm formation and gene expression of Bacteroides fragilis. *J Microbiol Biotechnol*. 2020;30:368-377.
13. Chen D, Jin D, Huang S, et al. *Clostridium butyricum*, a butyrate-producing probiotic, inhibits intestinal tumor development through modulating Wnt signaling and gut microbiota. *Cancer Lett*. 2020;469:456-467.
14. Li H, Xu M, Xu X, et al. Faecalibacterium prausnitzii Attenuates CKD via Butyrate-Renal GPR43 Axis. *Circ Res*. 2022;131:e120-e134.
15. Liu M, Xie W, Wan X, Deng T. *Clostridium butyricum* modulates gut microbiota and reduces colitis associated colon cancer in mice. *Int Immunopharmacol*. 2020;88:106862.
16. Zhou M, Yuan W, Yang B, Pei W, Ma J, Feng Q. *Clostridium butyricum* inhibits the progression of colorectal cancer and alleviates intestinal inflammation via the myeloid differentiation factor 88 (MyD88)-nuclear factor-kappa B (NF-kappaB) signaling pathway. *Ann Transl Med*. 2022;10:478.
17. Xiao Y, Dai X, Li K, Gui G, Liu J, Yang H. *Clostridium butyricum* partially regulates the development of colitis-associated cancer through miR-200c. *Cell Mol Biol*. 2017;29:59-66.
18. Lu S, Han L, Hu X, et al. N6-methyladenosine reader IMP2 stabilizes the ZFAS1/OLA1 axis and activates the Warburg effect: implication in colorectal cancer. *J Hematol Oncol*. 2021;14:188.
19. Shen C, Xuan B, Yan T, et al. m(6)A-dependent glycolysis enhances colorectal cancer progression. *Mol Cancer*. 2020;19:72.
20. Wang S, Gao S, Zeng Y, et al. N6-Methyladenosine reader YTHDF1 promotes ARHGEF2 translation and RhoA signaling in colorectal cancer. *Gastroenterology*. 2022;162:1183-1196.
21. Liu X, Liu L, Dong Z, et al. Expression patterns and prognostic value of m 6 A-related genes in colorectal cancer. *Am J Transl Res*. 2019;11:3972-3991.
22. Li T, Hu PS, Zuo Z, et al. METTL3 facilitates tumor progression via an m(6)A-IGF2BP2-dependent mechanism in colorectal carcinoma. *Mol Cancer*. 2019;18:112.
23. Peng W, Li J, Chen R, et al. Upregulated METTL3 promotes metastasis of colorectal cancer via miR-1246/SPRED2/MAPK signaling pathway. *J Exp Clin Cancer Res*. 2019;38:393.
24. Li M, Xia M, Zhang Z, et al. METTL3 antagonizes 5-FU chemotherapy and confers drug resistance in colorectal carcinoma. *Int J Oncol*. 2022;61:106.
25. Matsuyama T, Ishikawa T, Takahashi N, et al. Transcriptomic expression profiling identifies ITGBL1, an epithelial to mesenchymal transition (EMT)-associated gene, is a promising recurrence prediction biomarker in colorectal cancer. *Mol Cancer*. 2019;18:19.
26. Liu H, Li D, Sun L, et al. Interaction of lncRNA MIR100HG with hnRNPA2B1 facilitates m(6)A-dependent stabilization of TCF7L2 mRNA and colorectal cancer progression. *Mol Cancer*. 2022;21:74.
27. Colangelo T, Carbone A, Mazzarelli F, et al. Loss of circadian gene timeless induces EMT and tumor progression in colorectal cancer via Zeb1-dependent mechanism. *Cell Death Differ*. 2022;29:1552-1568.
28. Chen C, Yuan W, Zhou Q, et al. N6-methyladenosine-induced circ1662 promotes metastasis of colorectal cancer by accelerating YAP1 nuclear localization. *Theranostics*. 2021;11:4298-4315.
29. Zeng D, Zhou P, Jiang R, et al. Evodiamine inhibits vasculogenic mimicry in HCT116 cells by suppressing hypoxia-inducible

factor 1-alpha-mediated angiogenesis. *Anti-Cancer Drugs*. 2021;32:314-322.
30. Liang Z, Liu H, Zhang Y, et al. Cyr61 from adipose-derived stem cells promotes colorectal cancer metastasis and vasculogenic mimicry formation via integrin alphaV beta5. *Mol Oncol*. 2021;15:3447-3467.
31. Song X, An Y, Chen D, et al. Microbial metabolite deoxycholic acid promotes vasculogenic mimicry formation in intestinal carcinogenesis. *Cancer Sci*. 2022;113:459-477.
32. Chen H, Gao S, Liu W, et al. RNA N(6)-Methyladenosine methyltransferase METTL3 facilitates colorectal cancer by activating the m(6)A-GLUT1-mTORC1 Axis and is a therapeutic target. *Gastroenterology*. 2021;160:1284-1300.e16.
33. Chen S, Zhang L, Li M, et al. Fusobacterium nucleatum reduces METTL3-mediated m(6)a modification and contributes to colorectal cancer metastasis. *Nat Commun*. 2022;13:1248.
34. Zheng Y, Wang Y, Liu Y, et al. N6-Methyladenosine modification of PTTG3P contributes to colorectal cancer proliferation via YAP1. *Front Oncol*. 2021;11:669731.
35. Song P, Feng L, Li J, et al. Beta-catenin represses miR455-3p to stimulate m6A modification of HSF1 mRNA and promote its translation in colorectal cancer. *Mol Cancer*. 2020;19:129.
36. Chen H, Pan Y, Zhou Q, et al. METTL3 inhibits anti-tumor immunity by targeting m(6)A-BHLHE41-CXCL1/CXCR2 axis to promote colorectal cancer. *Gastroenterology*. 2022;21:60.
37. Zhou D, Tang W, Xu Y, et al. METTL3/YTHDF2 m6A axis accelerates colorectal carcinogenesis through epigenetically suppressing YPEL5. *Mol Oncol*. 2021;15:2172-2184.
38. Xiong J, He J, Zhu J, et al. Lactylation-driven METTL3-mediated RNA m(6)a modification promotes immunosuppression of tumor-infiltrating myeloid cells. *Mol Cell*. 2022;82:1660-1677.
39. Huang Y, Luo Y, Ou W, et al. Exosomal lncRNA SNHG10 derived from colorectal cancer cells suppresses natural killer cell cytotoxicity by upregulating INHBC. *Cancer Cell Int*. 2021;21:528.
40. Zhang H, Fang Z, Guo Y, Wang D. Long noncoding RNA SNHG10 promotes colorectal cancer cells malignant progression by targeting miR-3690. *Bioengineered*. 2021;12:6010-6020.
41. Zhang G, Wang T, Huang Z, et al. METTL3 dual regulation of the stability of LINC00662 and VEGFA RNAs promotes colorectal cancer angiogenesis. *Discov Oncol*. 2022;13:89.
42. Yu T, Liu J, Wang Y, et al. METTL3 promotes colorectal cancer metastasis by stabilizing PLAU mRNA in an m6A-dependent manner. *Biochem Biophys Res Commun*. 2022;614:9-16.
43. Tang J, Huang M, Peng H, et al. METTL3-mediated Hsa_circ_0000390 downregulation enhances the proliferation, migration, and invasion of colorectal cancer cells by increasing Notch1 expression. *Hum Cell*. 2023;36:703-711.
44. Yang J, Antin P, Berx G, et al. Guidelines and definitions for research on epithelial-mesenchymal transition. *Nat Rev Mol Cell Biol*. 2020;21:341-352.
45. Bracken C, Goodall GJ. The many regulators of epithelial-mesenchymal transition. *Nat Rev Mol Cell Biol*. 2022;23:89-90.
46. Tsai J, Yang J. Epithelial-mesenchymal plasticity in carcinoma metastasis. *Genes Dev*. 2013;27:2192-2206.
47. Jung H, Fattet L, Tsai J, et al. Apical-basal polarity inhibits epithelial-mesenchymal transition and tumour metastasis by PAR-complex-mediated SNAI1 degradation. *Nat Cell Biol*. 2019;21:359-371.
48. Zhang S, Chen H, Liu W, et al. miR-766-3p targeting BCL9L suppressed tumorigenesis, epithelial-mesenchymal transition, and metastasis through the beta-catenin signaling pathway in osteosarcoma cells. *Front Cell Dev Biol*. 2020;8:594135.
49. Wang W, Fang D, Zhang H, et al. Sodium butyrate selectively kills cancer cells and inhibits migration in colorectal cancer by targeting Thioredoxin-1. *Onco Targets Ther*. 2020;13:4691-4704.
50. Xu Q, Lu X, Li J, et al. Fusobacterium nucleatum induces excess methyltransferase-like 3-mediated microRNA-4717-3p maturation to promote colorectal cancer cell proliferation. *Cancer Sci*. 2022;113:3787-3800.
51. Lu X, Xu Q, Tong Y, et al. Long non-coding RNA EVADR induced by fusobacterium nucleatum infection promotes colorectal cancer metastasis. *Cell Rep*. 2022;40:111127.
52. Yamane T, Kanamori Y, Sawayama H, et al. Iron accelerates fusobacterium nucleatum-induced CCL8 expression in macrophages and is associated with colorectal cancer progression. *JCI Insight*. 2022;22:e156802.
53. Kong C, Liang L, Liu G, et al. Integrated metagenomic and metabolomic analysis reveals distinct gut-microbiome-derived phenotypes in early-onset colorectal cancer. *Gut*. 2022;11:gutjnl-2022-327156.
54. Zheng D, Dong X, Pan P, et al. Phage-guided modulation of the gut microbiota of mouse models of colorectal cancer augments their responses to chemotherapy. *Nat Biomed Eng*. 2019;3:717-728.
55. Zong X, Wang H, Xiao X, et al. Enterotoxigenic Escherichia coli infection promotes enteric defensin expression via FOXO6-METTL3-m(6)A-GPR161 signalling axis. *RNA Biol*. 2021;18:576-586.
56. McMurdie P, Stoeva M, Justice N, et al. Increased circulating butyrate and ursodeoxycholate during probiotic intervention in humans with type 2 diabetes. *BMC Microbiol*. 2022;22:19.

**How to cite this article:** Zhang K, Dong Y, Li M, et al. *Clostridium butyricum* inhibits epithelial–mesenchymal transition of intestinal carcinogenesis through downregulating METTL3. *Cancer Sci*. 2023;114:3114-3127. doi:10.1111/cas.15839